Clément M. Gosselin
Jing Wang

Département de Génie Méchanique
Université Laval
Québec, Canada
gosselin@gmc.ulaval.ca
wjing00@gmc.ulaval.ca

Singularity Loci of a Special Class of Spherical Three-degree-of-freedom Parallel Mechanisms with Revolute Actuators

Abstract

In this paper, we study the singularity loci of a special class of spherical three-degree-of-freedom parallel manipulators. The concise analytical expressions describing the singularity loci are obtained in the joint and in the Cartesian spaces by using the direct and inverse kinematic solutions of these manipulators, respectively. As mentioned elsewhere, there are three different types of singularities for parallel manipulators, each having a different physical interpretation. These types are considered and it is shown that, for the manipulators considered here, the three types of singularities coincide. Moreover, for the two types of manipulators studied here, there are only four singular configurations in the Cartesian space. In addition, the three-dimensional graphical representations of the singularity loci in the joint and in the Cartesian spaces are illustrated. The description of the singular configurations provided here has great significance for robot trajectory planning and control.

KEY WORDS—parallel mechanism, spherical parallel mechanism, spherical parallel manipulator, singularity, singularity loci, Jacobian matrix

1. Introduction

With the development of parallel robot technology, various types of three-degree-of-freedom (3-DoF) parallel manipulators have attracted the attention of researchers. According to their kinematic structure, 3-DoF parallel manipulators are usually of three types: planar, spherical and spatial. Hunt (1983) proposed various kinematic structures for parallel robots, an important one of which is the spatial 3-DoF 3-RPS parallel platform mechanism. This has two rotational and one translational degrees of freedom and has been widely researched (Agrawal 1991; Fang and Huang 1997; Lee and Shah 1987; Lee and Arjuman 1991; Pfreundschuh, Kumar, and Sugar 1991; Song and Zhang 1995; Waldron, Raghavan and Roth 1989). Planar and spherical parallel manipulators have been studied (Asada and Cro Granito 1985; Cox and Tesar 1989; Gosselin, Sefrioui and Richard 1992; Gosselin and Lavoie 1993; Gosselin, Lemieux and Merlet 1996). Recently, many other novel 3-DoF parallel manipulators have also been proposed, for example by Carretero et al. (2000) and Vischer and Clavel (2000). In this paper we are mainly concerned with studying a special class of spherical 3-DoF parallel mechanisms with revolute actuators and orthogonal axes. A prototype of such a manipulator was presented by Gosselin and Hamel (1994), where a high-performance camera-orienting device, also termed "agile eye," was introduced.

It is well known that singular configurations are inherent to mechanical systems and have serious influences on their properties. Therefore, these special configurations of the system are usually avoided in the design and application of mechanisms. Gosselin and Angeles (1990) have identified all types of singularities for parallel manipulators. Using this method, the singularity loci of simple 2-DoF and 3-DoF planar manipulators have been obtained (Sefrioui and Gosselin 1993, Sefrioui and Gosselin 1995, Gosselin and Wang 1997, Bonev and Gosselin 2001). For spherical 3-DoF parallel manipulators with prismatic actuators, the expression for the singularity loci has been provided (Sefrioui and Gosselin 1994).

In this paper, we study the representation of the singularity loci of two spherical 3-DoF parallel manipulators with revolute actuators and orthogonal axes. According to the analysis of Gosselin and Angeles (1990), there are three types of singularities for parallel manipulators. For the types of manipulators studied here, using the method presented by Gosselin and Angeles (1990), we derive the conditions for the three

The International Journal of Robotics Research
Vol. 21, No. 7, July 2002, pp. 649-659,

types of singularities in the joint and in the Cartesian spaces based on the direct and inverse kinematic solutions. These expressions are then used to construct the singularity loci. Finally, the results of the singular analysis of these two 3-DoF spherical manipulator are almost same.

2. A Special Class of Spherical 3-DoF Parallel Manipulator

The architecture of the most general spherical 3-DoF parallel manipulator was studied by Craver (1989), as a robotic shoulder module. As shown in Figure 1, it consists of a platform connected to a fixed base via three kinematic chains. Each of the chains is composed of two intermediate links and three revolute joints. The structure of the manipulator is such that the axes of all nine revolute joints intersect at one common point, which is the center of rotation of the mechanism. The three motors of the manipulator are fixed to the base, and the revolute joints connecting each of the three chains to the base are actuated. The unit vectors directed along the axes of the actuators are denoted by $\mathbf{u}_i$, $i = 1, 2, 3$, while the unit vectors directed along the axes of the revolute joints on the end effector are denoted by $\mathbf{v}_i$, $i = 1, 2, 3$. Finally, the unit vectors defined along the axes of the intermediate joints are denoted by $\mathbf{w}_i$, $i = 1, 2, 3$. The link angles are assumed to be identical on each of the kinematic chains connecting the base to the platform and are denoted by α_1 and α_2. Additionally, the platform and the base are assumed to be symmetric and the angle between the fixed axes is denoted by γ_1 while the angle between the axes on the platform is denoted by γ_2. When the architecture parameters are taken as $\alpha_1 = \alpha_2 = \gamma_1 = \gamma_2 = \pi/2$, the spherical parallel manipulator with the special geometry studied here is obtained, as shown in Figure 2. For this special spherical manipulator, called the agile eye, the unit vectors $\mathbf{u}_i$, $i = 1, 2, 3$, and the unit vectors $\mathbf{v}_i$, $i = 1, 2, 3$, define an orthogonal reference frame on the base and on the platform, respectively. We take the orthogonal frame defined by the three unit vectors $\mathbf{u}_i$, $i = 1, 2, 3$, as the fixed reference frame, i.e.,

$$\mathbf{u}_1 = [1, 0, 0]^T, \quad \mathbf{u}_2 = [0, 0, 1]^T, \quad \mathbf{u}_3 = [0, 1, 0]^T \tag{1}$$

The origin of the coordinate frame is at the center of rotation. The actuator angles are denoted by θ_i, $i = 1, 2, 3$, and are measured along the fixed axes defined by vectors $\mathbf{u}_i$, i=1,2,3, with respect to the fixed frame. Hence, the vectors along the intermediate joints can be written as

$$\mathbf{w}_1 = \begin{bmatrix} 0 \\ -s\theta_1 \\ c\theta_1 \end{bmatrix}, \quad \mathbf{w}_2 = \begin{bmatrix} -s\theta_2 \\ c\theta_2 \\ 0 \end{bmatrix}, \quad \mathbf{w}_3 = \begin{bmatrix} c\theta_3 \\ 0 \\ -s\theta_3 \end{bmatrix}. \tag{2}$$

As shown in Gosselin and Lavoie (1993), this special architecture leads to an isotropic Jacobian in the reference configurations shown in Figure 2. It was also shown in Gosselin and Gagné (1995) that this special architecture leads to a closed-form solution of the direct kinematic problem.

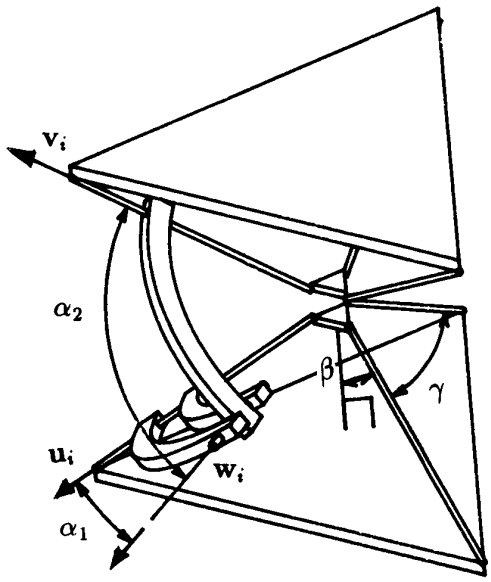

Fig. 1. A general class of 3-DoF spherical parallel manipulator.

3. Kinematic Analysis

Because both the direct and the inverse kinematic problems have already been solved for this special kind of architecture in Gosselin and Gagné (1995), we now only briefly outline the results obtained for the kinematic analysis. The notation used here is the same as that used in Gosselin and Gagné (1995).

3.1. Inverse Kinematics

For this special spherical manipulator with revolute actuators, the solution of the inverse kinematic problem is very simple and leads to a maximum of eight real solutions. We can use the following geometric constraints

$$\mathbf{w}_i \cdot \mathbf{v}_i = 0 \qquad i = 1, 2, 3. \tag{3}$$

When the orientation of the end effector is given, we then have two solutions for θ_i for each leg, namely

$$\tan\theta_1 = \frac{v_{1z}}{v_{1y}}, \qquad \tan\theta_2 = \frac{v_{2y}}{v_{2x}}, \qquad \tan\theta_3 = \frac{v_{3x}}{v_{3z}}, \tag{4}$$

where v_{ix}, v_{iy} and v_{iz} are, respectively, the x, y and z components of vector $\mathbf{v}_i$.

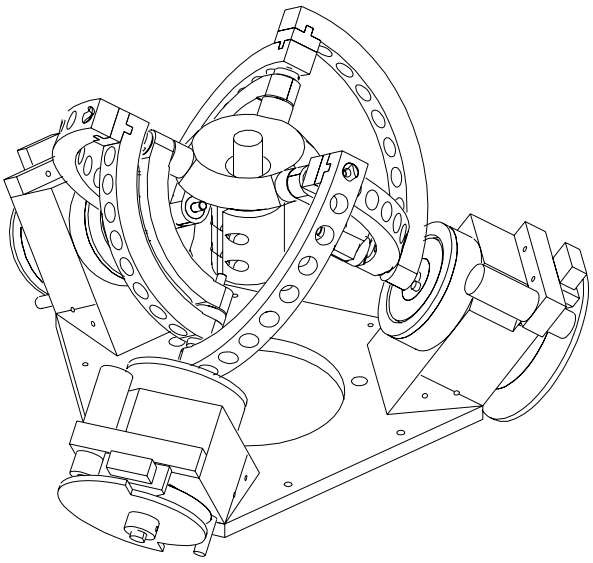

Fig. 2. A special class of 3-DoF spherical parallel manipulators with revolute actuators.

3.2. Direct Kinematics

In Gosselin and Gagné (1995), the direct kinematic problem associated with the particular geometry of the spherical 3-DoF parallel manipulator studied here has been solved successfully and closed-form solutions have been obtained. This is due to the decoupling of the solutions into two groups, each of which has four solutions. The first set of solutions is

$$\begin{aligned} \phi_1 &= -\theta_2 \\ \phi_2 &= \tan^{-1}\left(\frac{-C_1}{C_2}\right) \\ \phi_3 &= \tan^{-1}\left(\frac{-A_1}{B_1}\right) = \tan^{-1}\left(\frac{-A_2}{B_2}\right), \end{aligned} \tag{5}$$

where

$$\begin{aligned} C_1 &= \cos\phi_1 \sin\phi_1 \sin\theta_1 \cos\theta_3 + \cos\theta_1 \sin\theta_3 \\ C_2 &= \cos\phi_1 \cos\theta_1 \cos\theta_3 - \sin\phi_1 \sin\theta_1 \sin\theta_3 \\ A_1 &= \cos\phi_1 \sin\theta_1 \\ B_1 &= \cos\phi_2 \cos\theta_1 - \sin\phi_1 \sin\phi_2 \sin\theta_1 \\ A_2 &= \cos\phi_1 \sin\phi_2 \cos\theta_3 + \cos\phi_2 \sin\theta_3 \\ B_2 &= -\sin\phi_1 \cos\theta_3. \end{aligned} \tag{6}$$

The second set of solutions is

$$\phi_2 = \tfrac{\pi}{2}, \qquad \phi_1 = \pm\tfrac{\pi}{2} - \phi_3 \tag{7}$$

$$\phi_2 = -\tfrac{\pi}{2}, \qquad \phi_1 = \pm\tfrac{\pi}{2} + \phi_3, \tag{8}$$

where $\phi_i, i = 1, 2, 3$, are the Euler angles used to describe the orientation of the platform and these are defined according to a convention involving successive rotations about the Z, Y and X axes. According to this convention, matrix $\mathbf{Q}$, representing the orientation of the platform with respect to the fixed frame, can be written as

$$\mathbf{Q} = \begin{bmatrix} c_1c_2 & c_1s_2s_3 + s_1c_3 & -c_1s_2c_3 + s_1s_3 \\ -s_1c_2 & -s_1s_2s_3 + c_1c_3 & s_1s_2c_3 + c_1s_3 \\ s_2 & -c_2s_3 & c_2c_3 \end{bmatrix}, \tag{9}$$

where c_i and s_i represent $\cos\phi_i$ and $\sin\phi_i$. Although they lead to formulation singularities, Euler angles are used here because they drastically reduce the algebraic complexity of the direct kinematic solution. Moreover, formulation singularities are easily handled, as seen in a following section.

4. Singularity Analysis

Gosselin and Angeles (1990) have presented a general classification of the different types of singularities occurring in closed kinematic chains based on two Jacobian matrices, $\mathbf{A}$ and $\mathbf{B}$. They have identified three types of singularities and have given their different physical interpretations. This classification was further refined by Zlatanov, Fenton, and Benhabib (1994). In this paper, we study the singularity loci associated with the three types of singularities of the spherical 3-DoF parallel manipulator with particular geometry.

Following the formalism proposed in Gosselin and Angeles (1990) for parallel manipulators, two Jacobian matrices $\mathbf{A}$ and $\mathbf{B}$ are obtained and the velocity equations can be written as

$$\mathbf{A}\boldsymbol{\omega} + \mathbf{B}\dot{\boldsymbol{\theta}} = 0, \tag{10}$$

where $\dot{\boldsymbol{\theta}}$ is the vector of actuated joint rates and $\boldsymbol{\omega}$ is the angular velocity vector of the end effector. For a 3-DoF spherical parallel manipulator, matrices $\mathbf{A}$ and $\mathbf{B}$ are given by Gosselin and Angeles (1989), and can be written as

$$\mathbf{A} = \begin{bmatrix} (\mathbf{w}_1 \times \mathbf{v}_1)^T \\ (\mathbf{w}_2 \times \mathbf{v}_2)^T \\ (\mathbf{w}_3 \times \mathbf{v}_3)^T \end{bmatrix} \tag{11}$$

and

$$\mathbf{B} = \mathrm{diag}(\mathbf{w}_1 \times \mathbf{u}_1 \cdot \mathbf{v}_1, \mathbf{w}_2 \times \mathbf{u}_2 \cdot \mathbf{v}_2, \mathbf{w}_3 \times \mathbf{u}_3 \cdot \mathbf{v}_3). \tag{12}$$

For the spherical parallel manipulator with the special orthogonal geometry, the expression of the vectors $\mathbf{u}_i$, $\mathbf{w}_i$ and $\mathbf{v}_i$ are given by Gosselin and Gagné (1995). Vectors $\mathbf{u}_i$ are given in eq. (1), vectors $\mathbf{w}_i$ in eq. (2) and vectors $\mathbf{v}_i$ are written as

$$\begin{aligned} \mathbf{v}_1 &= [-c_1s_2s_3 - s_1c_3, s_1s_2s_3 - c_1c_3, c_2s_3]^T \\ \mathbf{v}_2 &= [-c_1c_2, s_1c_2, -s_2]^T \\ \mathbf{v}_3 &= [c_1s_2c_3 - s_1s_3, -s_1s_2c_3 - c_1s_3, -c_2c_3]^T, \end{aligned} \tag{13}$$

where c_i and s_i represent $\cos\phi_i$ and $\sin\phi_i$.

4.1. The First Type of Singularity

The first type of singularity occurs when $\det(\mathbf{B}) = 0$. In this case, the end effector of the manipulator loses one or more degrees of freedom and lies in a deadpoint position. The corresponding configuration belongs to the boundary of the workspace. From eq. (12) the condition for this type of singularity can be obtained, i.e.,

$$p_i = (\mathbf{w}_i \times \mathbf{u}_i) \cdot \mathbf{v}_i = 0, \qquad i = 1, 2, 3. \tag{14}$$

From the above equation, geometrically, it is clear that this type of singularity arises when the vectors $\mathbf{u}_i$, $\mathbf{w}_i$ and $\mathbf{v}_i$ are coplanar, i.e., the corresponding leg is totally unfolded or folded. The end effector lies on the boundary of the workspace. In this special configuration, the gripper can resist one or more moments without exerting any torque at the actuated joints.

Algebraically, substituting eqs. (1), (2) and (13) into eq. (14), three equations containing input angles θ_i and output angles ϕ_i for $i = 1, 2, 3$, can be obtained, namely

$$\begin{aligned} p_1 &= c\theta_1(-c_1c_3 + s_1s_2s_3) + s\theta_1c_2s_3 \\ p_2 &= -c\theta_2c_1c_2 + s\theta_2s_1c_2 \\ p_3 &= s\theta_3(-s_1s_3 + c_1s_2c_3) - c\theta_3c_2c_3. \end{aligned} \tag{15}$$

4.1.1. Singularity Loci in the Joint Space

The substitution of eq. (5), i.e., the first set of direct kinematic solutions, into eq. (15) then leads to

$$\begin{aligned} p_1 &= -\frac{c\theta_1c\theta_2c\theta_3 + s\theta_1s\theta_2s\theta_3}{\sqrt{(1 - c\theta_2^2 + c\theta_1^2c\theta_2^2)(1 - c\theta_1^2 + c\theta_1^2c\theta_3^2)}} \\ p_2 &= -\frac{c\theta_1c\theta_2c\theta_3 + s\theta_1s\theta_2s\theta_3}{\sqrt{(1 - c\theta_2^2 + c\theta_1^2c\theta_2^2)(1 - c\theta_3^2 + c\theta_2^2c\theta_3^2)}} \\ p_3 &= -\frac{c\theta_1c\theta_2c\theta_3 + s\theta_1s\theta_2s\theta_3}{\sqrt{(1 - c\theta_3^2 + c\theta_2^2c\theta_3^2)(1 - c\theta_1^2 + c\theta_1^2c\theta_3^2)}}. \end{aligned} \tag{16}$$

From eq. (16), the representation of the singularity loci corresponding to the first set of direct kinematic solutions in the joint space is therefore obtained as

$$c\theta_1c\theta_2c\theta_3 + s\theta_1s\theta_2s\theta_3 = 0. \tag{17}$$

The latter condition states that this type of singularity will occur in the joint space when the three input angles θ_1, θ_2 and θ_3 satisfy eq. (17). Since the surface represented by eq. (17) depends only on the three input angles, the singularity loci can be plotted in the joint space $(\theta_1, \theta_2, \theta_3)$, as shown in Figure 3. It can be shown that the singularity loci have a period of π. The planar representation of the singular surface will be illustrated in order to better describe the singularity loci. By symmetry, one of the input angles may be fixed; the first input angle θ_1 is fixed here. A plot of the value of θ_3 as a function of the value of θ_2 is represented in Figure 4, with $\theta_1 \in [-\pi/2\ \pi/2]$. When θ_1 is equal to zero or $\pm\pi/2$ the singularity loci are the straight lines in Figure 4 and the planes in Figure 3.

The substitution of the second set of direct kinematic solutions, i.e., eqs. (7) and (8) into eq. (15), leads to

$$p_1 = p_2 = p_3 = 0. \tag{18}$$

This means that when the mobile platform is in one of the four configurations corresponding to the four solutions of the second set of direct kinematic solutions, the end effector of this manipulator lies on the boundary of the workspace. In other words, the second set of four solutions always corresponds to singular configurations. It also states that this manipulator has only four useful direct kinematic solutions among the eight algebraic solutions. In fact, this result has been pointed out by Gosselin and Gagné (1995). Hence, the singularity condition for this type of manipulator in the joint space is eq. (17).

4.1.2. Singularity Loci in the Cartesian Space

The substitution of eq. (4), i.e., the solution of the inverse kinematic problem into eq. (15) leads to

$$\begin{aligned} p_1 &= \sqrt{T - c_1^2c_2^2c_3^2 + c_1^2c_2^2} \\ p_2 &= c_2 \\ p_3 &= \sqrt{T - c_1^2c_2^2c_3^2 + c_2^2c_3^2}, \end{aligned} \tag{19}$$

where

$$T = 1 + 2c_1^2c_3^2 - c_1^2 - c_3^2 - 2s_1s_2s_3c_1c_3. \tag{20}$$

From eq. (19), the condition for the first type of singularity in the Cartesian space is obtained, i.e.

$$c_2 = 0. \tag{21}$$

It is clear that this condition is the same as the second set of direct kinematic solutions. In such a situation, solutions for the four rotation matrices $\mathbf{Q}$ are obtained. These cases correspond to four orientations of the mobile platform, which are

$$\begin{aligned} &\begin{cases} \mathbf{v}_1 = -\mathbf{u}_1 \\ \mathbf{v}_2 = -\mathbf{u}_2 \\ \mathbf{v}_3 = -\mathbf{u}_3 \end{cases}, \quad \begin{cases} \mathbf{v}_1 = \mathbf{u}_1 \\ \mathbf{v}_2 = -\mathbf{u}_2 \\ \mathbf{v}_3 = \mathbf{u}_3 \end{cases}, \\ &\begin{cases} \mathbf{v}_1 = -\mathbf{u}_1 \\ \mathbf{v}_2 = \mathbf{u}_2 \\ \mathbf{v}_3 = \mathbf{u}_3 \end{cases}, \quad \begin{cases} \mathbf{v}_1 = \mathbf{u}_1 \\ \mathbf{v}_2 = \mathbf{u}_2 \\ \mathbf{v}_3 = -\mathbf{u}_3 \end{cases}. \end{aligned} \tag{22}$$

In each case, the $\mathbf{u}_i$ and $\mathbf{v}_i$ vectors of each leg are aligned. For the first condition of eq. (22), the directions of the three vectors $\mathbf{u}_i$ are in the opposite sense of $\mathbf{v}_i$, respectively, as shown in Figure 5. In the other three cases, only one pair of the three vectors oppose each other in direction. Since this spherical manipulator is symmetric, the geometric representation corresponding to the last three cases is the same and is illustrated

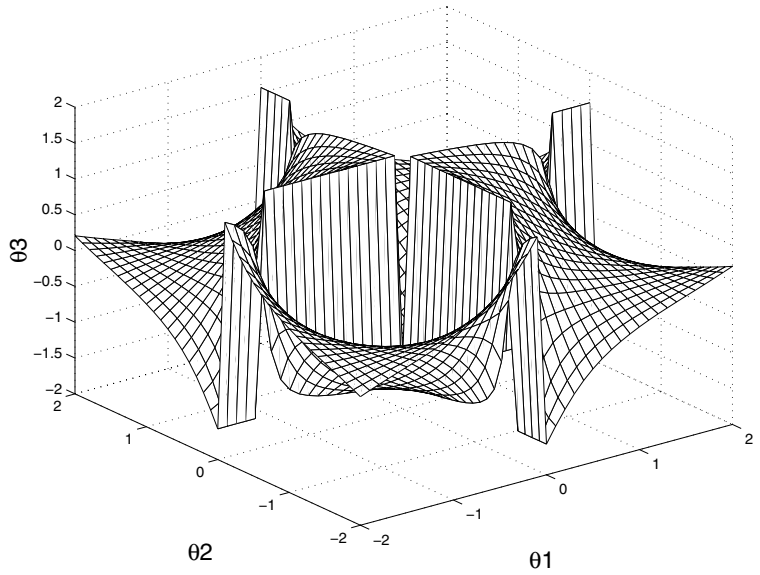

Fig. 3. Singularity loci of the 3-DoF spherical parallel manipulator with revolute actuators in the joint space.

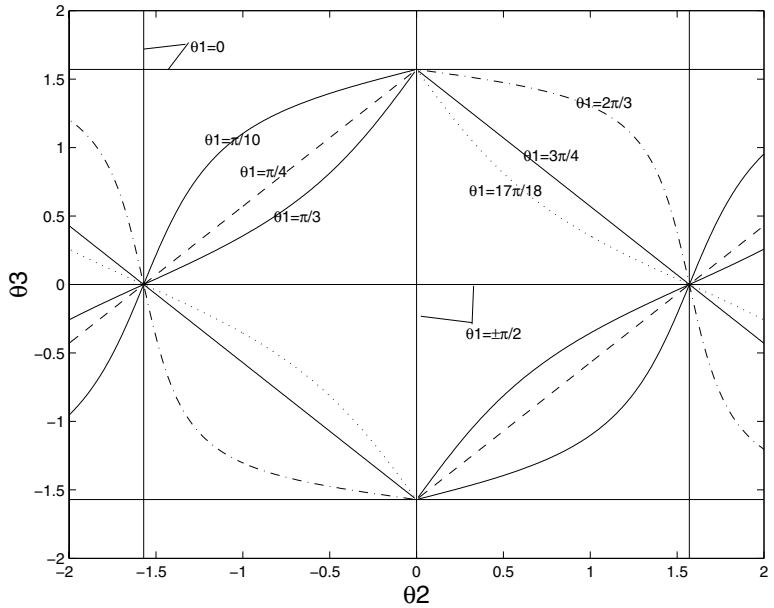

Fig. 4. Planar representation of singularity loci of the 3-DoF spherical parallel manipulator with revolute actuators in the joint space.

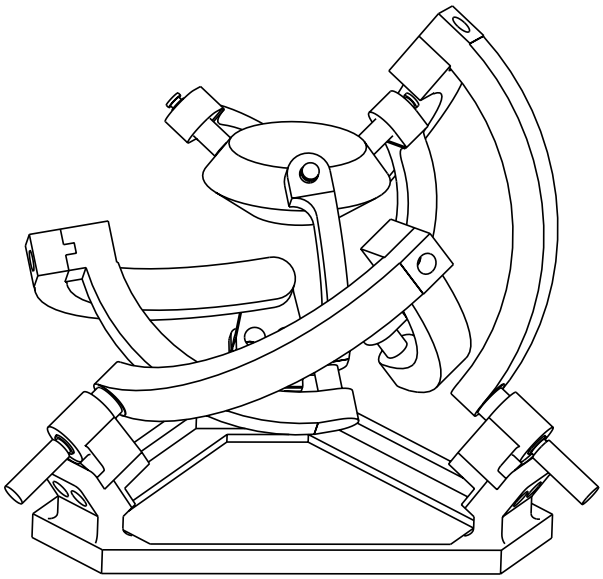

Fig. 5. First singular configuration of the special 3-DoF spherical parallel manipulator with revolute actuators.

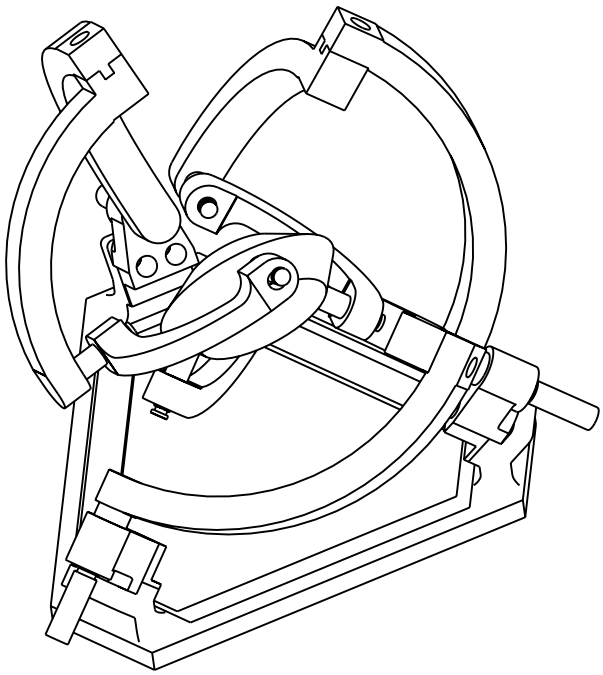

Fig. 6. Second singular configuration of the special 3-DoF spherical parallel manipulator with revolute actuators.

in Figure 6. When the platform is in one of these configurations, the actuators can be moved arbitrarily and will not affect the pose of the platform.

4.2. The Second Type of Singularity

The second type of singularity occurs when $\det(\mathbf{A}) = 0$. In general, as opposed to the first one, in this case, the end effector of the manipulator gains one or more degrees of freedom and the input link is at a deadpoint. The corresponding configuration may be located inside the workspace. Therefore, it is important to identify this type of singularity in robotic design and control.

4.2.1. Singularity Loci in the Joint Space

This type of singularity occurs when $\det(\mathbf{A}) = 0$. In general, in this special configuration, non-zero angular velocities of the gripper are possible even if the three input velocities are zero. Substituting eqs. (1), (2) and (13) into eq. (11), the expression for the matrix $\mathbf{A}$ as a function of the Euler angles ϕ_i and input angles θ_i for $i = 1, 2, 3$, can be obtained as

$$\mathbf{A} = \begin{bmatrix} a_{11} & a_{12} & a_{13} \\ a_{21} & a_{22} & a_{23} \\ a_{31} & a_{32} & a_{33} \end{bmatrix}, \tag{23}$$

where

$$\begin{aligned}
a_{11} &= -s\theta_1 c_2 s_3 + c\theta_1 c_1 c_3 - c\theta_1 s_1 s_2 s_3 \\
a_{12} &= -c\theta_1 s_1 c_3 - c\theta_1 c_1 s_2 s_3 \\
a_{13} &= -s\theta_1 s_1 c_3 - s\theta_1 c_1 s_2 s_3 \\
a_{21} &= -c\theta_2 s_2 \\
a_{22} &= -s\theta_2 s_2 \\
a_{23} &= -s\theta_2 s_1 c_2 + c\theta_2 c_1 c_2 \\
a_{31} &= -s\theta_3 c_1 s_3 - s\theta_3 s_1 s_2 c_3 \\
a_{32} &= s\theta_3 s_1 s_3 - s\theta_3 c_1 s_2 c_3 + c\theta_3 c_2 c_3 \\
a_{33} &= -c\theta_3 c_1 s_3 - c\theta_3 s_1 s_2 c_3,
\end{aligned} \tag{24}$$

where the notation is the same as in the previous section.

Using the first set of direct kinematic solutions, the determinant of matrix $\mathbf{A}$ can be obtained as

$$\det(\mathbf{A}) = -(c\theta_1 c\theta_2 c\theta_3 + s\theta_1 s\theta_2 s\theta_3). \tag{25}$$

Using the second set of solutions, the following expression for the determinant of matrix $\mathbf{A}$ is obtained

$$\det(\mathbf{A}) = c\theta_1 c\theta_2 c\theta_3 + s\theta_1 s\theta_2 s\theta_3. \tag{26}$$

From eqs. (25) and (26), we can conclude that if $\det(\mathbf{A}) = 0$, then the following expression will be equal to zero:

$$c\theta_1 c\theta_2 c\theta_3 + s\theta_1 s\theta_2 s\theta_3 = 0. \tag{27}$$

In other words, the two sets of solutions are equivalent for the purpose of determining the second type of singularity of the manipulator. It is noticed that this result is identical to the condition of the first type of singularity in the joint space. This situation has been analyzed in detail in the preceding section.

4.2.2. Singularity Loci in the Cartesian Space

Using the solution of the inverse kinematics, i.e., substituting eq. (4) into eq. (11), the determinant of matrix **A** can be obtained as

$$\det(\mathbf{A}) = \pm \frac{c_2 T}{\sqrt{T - c_1^2 c_2^2 c_3^2 + c_1^2 c_2^2}\sqrt{T - c_1^2 c_2^2 c_3^2 + c_2^2 c_3^2}}. \quad (28)$$

When $\det(\mathbf{A}) = 0$, eq. (28) has two distinct sets of solutions. These sets are obtained with

$$c_2 = 0 \quad \text{or} \quad T = 0. \quad (29)$$

In fact, these two solutions have the same geometric interpretation. The proof of this follows. Under the first condition of eq. (29), the mobile platform has only four singular orientations in the Cartesian space as mentioned above. The second condition of eq. (29) is now considered. Using trigonometric identities, the second condition of eq. (29) can be simplified as

$$T = 1 + c2\phi_1 c2\phi_3 - s2\phi_1 s\phi_2 s2\phi_3 = 0. \quad (30)$$

We can rewrite eq. (30) as

$$s\phi_2 = \frac{1 + c2\phi_1 c2\phi_3}{s2\phi_1 s2\phi_3}. \quad (31)$$

Since $|s\phi_2| \leq 1$, we can obtain the following condition

$$\left| \frac{1 + c2\phi_1 c2\phi_3}{s2\phi_1 s2\phi_3} \right| \leq 1. \quad (32)$$

The three cases are discussed separately below.

1. $s2\phi_1 s2\phi_3 > 0$
   In this case, eq. (32) can be rewritten as follows

   $$-s2\phi_1 s2\phi_3 \leq 1 + c2\phi_1 c2\phi_3 \leq s2\phi_1 s2\phi_3. \quad (33)$$

   We can simplify eq. (33) and obtain

   $$\cos(2\phi_1 + 2\phi_3) \leq -1 \quad \text{and} \quad \cos(2\phi_1 - 2\phi_3) \geq -1. \quad (34)$$

   Since the value of the cosine function is in the range $[-1, 1]$ this condition can be written as

   $$\cos(2\phi_1 + 2\phi_3) = -1 \quad (35)$$

   i.e., $\cos(\phi_1 + \phi_3) = 0$. This condition leads to

   $$\phi_1 + \phi_3 = \pm \frac{\pi}{2}. \quad (36)$$

   Consequently, substituting this condition into eq. (31), we can obtain $\sin\phi_2 = 1$.

2. $s2\phi_1 s2\phi_3 < 0$
   In this case, eq. (32) can be rewritten as follows

   $$s2\phi_1 s2\phi_3 \leq 1 + c2\phi_1 c2\phi_3 \leq -s2\phi_1 s2\phi_3. \quad (37)$$

   Similarly, the condition to be satisfied for this case is

   $$\cos(2\phi_1 - 2\phi_3) = -1, \quad (38)$$

   i.e., $\cos(\phi_1 - \phi_3) = 0$ or $\phi_1 - \phi_3 = \pm\frac{\pi}{2}$. Similarly, we can obtain $\sin\phi_2 = -1$.

3. $s2\phi_1 s2\phi_3 = 0$
   In this case, eq. (30) becomes

   $$c2\phi_1 c2\phi_3 = -1. \quad (39)$$

   and we can obtain the specific values for ϕ_1 and ϕ_3:

   $$\begin{aligned} &(\phi_1 = 0 \quad \text{and} \quad \phi_3 = \pm\frac{\pi}{2}) \quad \text{or} \\ &(\phi_3 = 0 \quad \text{and} \quad \phi_1 = \pm\frac{\pi}{2}). \end{aligned} \quad (40)$$

   From eq. (30), it seems that ϕ_2 can be any value. However, the three constraint conditions of this manipulator, i.e., eq. (3), have to be considered here. Then the condition to be satisfied for this case is only $c_2 = 0$. In other words, in this case, the three Euler angles ϕ_1, ϕ_2 and ϕ_3 all have specific values. Moreover, it is not difficult to detect that the third case is a special instance of cases one and two.

From the above analysis, when $\cos(\phi_1 + \phi_3) = 0$ or $\cos(\phi_1 - \phi_3) = 0$, i.e., $T = 0$, $c_2 = 0$ is obtained. Hence, we can say that the two conditions of eq. (29) are equivalent. In addition, if we directly consider the second group of direct kinematic solutions, the proof that conditions $c2 = 0$ and $T = 0$ are the same can be simpler. Therefore, $c_2 = 0$ is also the singular condition of the second type of singularity in the Cartesian space. The four orientations of the mobile platform corresponding to this case have been given in the preceding section.

4.3. The Third Type of Singularity

The third type of singularity occurs when both **A** and **B** are simultaneously singular. In this case, this manipulator becomes architecturally singular. This type of singularity demands that the architecture parameters of a manipulator satisfy certain special conditions. For the spherical manipulator studied here, from the discussion above we can see that when $(c\theta_1 c\theta_2 c\theta_3 + s\theta_1 s\theta_2 s\theta_3) = 0$ or $c_2 = 0$ the determinants of matrices **A** and **B** are equal to zero simultaneously. Moreover, the constraint equation given by eq. (3) degenerates.

4.4. Discussion

From the above singularity analysis, it is clear that, for the manipulator studied here, the singularity locus in the Cartesian space consists of four isolated configurations, given in eq. (22). In the Cartesian space, the singularity loci of type I, II and III coincide. Moreover, these four configurations correspond exactly to the second set of solutions of the direct kinematic problem, given in eqs. (7) and (8). The linear equations obtained in eqs. (7) and (8) are due to the formulation singularity of the Euler angles and these expressions correspond to only four configurations. Hence, when the platform is in one of these Cartesian orientations, all three actuators can be moved freely without any motion of the platform, i.e., these four Cartesian configurations can be mapped into the whole joint space. In order to escape this singularity of type III, one must move onto the singularity surface in the joint space (Figure 3) and then use an external force to move the platform out of the singular configuration.

The fact that the singularities are limited to isolated configurations in the Cartesian space is a special property of the architecture studied in this paper.

5. Singularity Analysis of the Argos Manipulator

Recently, a novel parallel spherical mechanism—referred to as the Argos mechanism—with three rotational degrees of freedom has been presented by Vischer and Clavel (2000) for use as a robot wrist. As shown in Figure 7, this mechanism consists of an end effector connected to the base by three identical kinematic chains. Each chain is attached to the base by a revolute joint with its axis pointing to the virtual rotation center. Each axis carries a pantograph. An S-joint links the pantograph to the end effector. The structure of the manipulator is such that all joints of one kinematic chain lie in a plane and the axis of the revolute joint and the vector pointing from the virtual rotation center to the S-joints of the end effector are orthogonal to each other. The virtual rotation center is chosen as the origin for the base frame as well as for the moving frame.

5.1. Kinematic Analysis

For the Argos mechanism, the solutions to the direct and inverse kinematic problems have been obtained by Vischer and Clavel (2000). In comparison with the mechanism studied above—the agile eye—it can be shown that the results of the kinematic problems associated with the two mechanisms are quite similar, although their structures are different. In addition, when studying the singularity loci of the Argos mechanism using the method described by Gosselin and Angeles (1990), it can be shown that the singularity loci for the Argos mechanism are similar to those obtained for the agile eye. We now briefly give the results of the singularity analysis for the

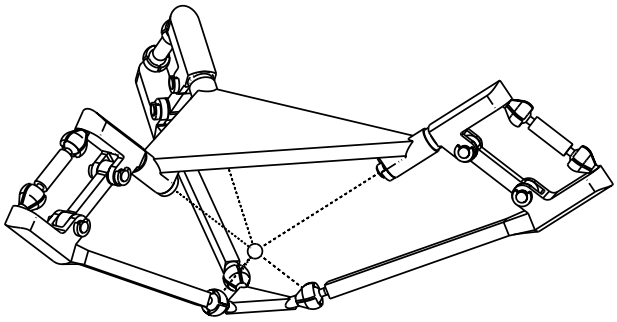

Fig. 7. The Argos mechanism.

Argos mechanism. The notation used here is the same as in the preceding section.

For the Argos mechanism, the expressions of the vectors $\mathbf{u}_i$, $\mathbf{w}_i$ and $\mathbf{v}_i$ are given in Vischer and Clavel (2000). These are

$$\mathbf{u}_1 = [1, 0, 0]^T, \quad \mathbf{u}_2 = [0, 1, 0]^T, \quad \mathbf{u}_3 = [0, 0, 1]^T \tag{41}$$

$$\mathbf{w}_1 = \begin{bmatrix} 0 \\ c\theta_1 \\ s\theta_1 \end{bmatrix}, \quad \mathbf{w}_2 = \begin{bmatrix} -c\theta_2 \\ 0 \\ s\theta_2 \end{bmatrix}, \quad \mathbf{w}_3 = \begin{bmatrix} -c\theta_3 \\ -s\theta_3 \\ 0 \end{bmatrix} \tag{42}$$

$$\begin{aligned} \mathbf{v}_1 &= [c_2, s_1 s_2, -s_2 c_1]^T \\ \mathbf{v}_2 &= [s_2 s_3, c_1 c_3 - s_1 c_2 s_3, s_1 c_3 + c_1 c_2 s_3]^T \\ \mathbf{v}_3 &= [-s_2 c_3, s_1 c_2 c_3 + c_1 s_3, s_1 s_3 - c_1 c_2 c_3]^T, \end{aligned} \tag{43}$$

where c_i and s_i represent $\cos\phi_i$ and $\sin\phi_i$ and ϕ_i, $i = 1, 2, 3$, are the Euler angles involving successive rotations about the X, Y and X axes.

For the Argos mechanism, due to the proper choice of the Euler angles, the direct and inverse kinematic problems were solved in closed-form, both having eight solutions.

5.1.1. Solution of the Inverse Kinematics

In Vischer and Clavel (2000), when the orientation of the end effector is given, the two solutions for the unknown joint angle θ_i for each chain are given as

$$\theta_i = \arctan 2(\pm a_i, \mp b_i), \quad i = 1, 2, 3, \tag{44}$$

where

$$a_1 = s_1 s_2, \tag{45}$$

$$b_1 = -c_1 s_2 \tag{46}$$

$$a_2 = -s_2 s_3, \tag{47}$$

$$b_2 = s_1 c_3 + c_1 c_2 s_3 \tag{48}$$

$$a_3 = s_2 c_3 \tag{49}$$

$$b_3 = -c_1 s_3 - s_1 c_2 c_3. \tag{50}$$

5.1.2. Solution of the Direct Kinematics

In Vischer and Clavel (2000), the first set of solutions of the direct kinematic problem of the Argos mechanism is given as

$$\begin{aligned}\phi_1 &= \theta_1\\ \phi_2 &= \tan^{-1}\left(\frac{-C_1}{C_2}\right)\\ \phi_3 &= \tan^{-1}\left(\frac{-A_1}{B_1}\right) = \tan^{-1}\left(\frac{-A_2}{B_2}\right),\end{aligned} \tag{51}$$

where

$$\begin{aligned}C_1 &= -c\theta_1 s\theta_2 c\theta_3 - s\theta_1 c\theta_2 s\theta_3\\ C_2 &= c\theta_2 c\theta_3 - c\theta_1 s\theta_1 s\theta_2 s\theta_3\\ A_1 &= s\theta_1 s\theta_2\\ B_1 &= -c\theta_2 s\phi_2 + c\theta_1 s\theta_2 c\phi_2\\ A_2 &= c\theta_3 s\phi_2 - s\theta_1 s\theta_3 c\phi_2\\ B_2 &= -c\theta_1 s\theta_3.\end{aligned} \tag{52}$$

The second set of solutions is

$$\begin{aligned}\phi_2 &= 0, \quad \phi_1 + \phi_3 = 0, \pi\\ \phi_2 &= \pi, \quad \phi_1 - \phi_3 = 0, \pi.\end{aligned} \tag{53}$$

5.2. Singularity Analysis

Similarly to the singularity analysis of the agile eye, the singularity loci of the Argos mechanism can be obtained.

5.2.1. The First Type of Singularity

The first type of singularity occurs when $\det(\mathbf{B}) = 0$. Substituting eqs. (41)–(43) into eq. (14), three equations containing input angles θ_i and output angles ϕ_i for $i = 1, 2, 3$, can be obtained:

$$\begin{aligned}p_1 &= s\theta_1 s_1 s_2 + c\theta_1 c_1 s_2\\ p_2 &= -c\theta_2(s_1 c_3 + c_1 c_2 s_3) - s\theta_2 s_2 s_3\\ p_3 &= c\theta_3(c_1 s_3 + s_1 c_2 c_3) + s\theta_3 s_2 c_3.\end{aligned} \tag{54}$$

1. Singularity loci in the joint space

   The substitution of eq. (52), i.e., the first set of direct kinematic solutions, into eq. (54) leads to the representation of the singularity loci of the Argos in the joint space as

   $$c\theta_1 s\theta_2 c\theta_3 + s\theta_1 c\theta_2 s\theta_3 = 0. \tag{55}$$

   Clearly, this condition is identical to what was obtained above for the agile eye. The substitution of the second set of direct kinematic solutions, i.e., eq. (53), into eq. (54) leads to

   $$p_1 = p_2 = p_3 = 0. \tag{56}$$

   This states that the four configurations of the end effector of this manipulator corresponding to the four solutions of the second set of direct kinematic solutions are always singular. It also proves that this manipulator has only four nonsingular direct kinematic solutions.

2. Singularity loci in the Cartesian space

   The substitution of eq. (44), i.e., the solution of the inverse kinematic problem, into eq. (14) leads to

   $$\begin{aligned}p_1 &= s_2\\ p_2 &= -\sqrt{T + s_2^2(1 + c_1^2 c_3^2 - c_1^2 - c_3^2)}\\ p_3 &= \sqrt{T + c_1^2 s_2^2 c_3^2},\end{aligned} \tag{57}$$

   where

   $$T = -2c_1^2 c_3^2 + c_1^2 + c_3^2 + 2c_1 c_2 c_3 s_1 s_3. \tag{58}$$

   It is apparent that the condition for the first type of singularity in the Cartesian space is

   $$s\phi_2 = 0. \tag{59}$$

   In such a situation, the four orientations of the end effector corresponding to the second set of the direct solutions are the same as for the agile eye, i.e., eq. (22). As mentioned in Vischer and Clavel (2000), if one of the S-joints lies on its corresponding motor axis, the pantograph can be freely moved without influencing the orientation of the end effector. That is, when all three S-joints lie on their corresponding motor axes, any set of motor angles can be freely imposed.

5.2.2. The Second Type of Singularity

The second type of singularity occurs when $\det(\mathbf{A}) = 0$.

1. Singularity loci in the joint space

   Using the first set of direct kinematic solutions, the determinant of matrix $\mathbf{A}$ can be obtained as

   $$\det(\mathbf{A}) = -(c\theta_1 s\theta_2 c\theta_3 + s\theta_1 c\theta_2 s\theta_3). \tag{60}$$

   Using the second set of solutions then leads to the following expression for the determinant of matrix $\mathbf{A}$

   $$\det(\mathbf{A}) = c\theta_1 s\theta_2 c\theta_3 + s\theta_1 c\theta_2 s\theta_3. \tag{61}$$

   Similarly to the agile eye, the condition for the second type of singularity of the Argos mechanism is identical to the condition of the first type of singularity in the joint space.

2. Singularity loci in the Cartesian space

   Substituting the solution of the inverse kinematic problem into eq. (11), the condition of the determinant of matrix **A** being zero can be obtained as

$$s_2 = 0 \quad \text{or} \quad T = 0. \tag{62}$$

   Using the same method as in section 4.2.2, we can prove that these two solutions have the same geometric interpretation. Therefore, $s_2 = 0$ is the condition for the second type of singularity in the Cartesian space.

5.2.3. The Third Type of Singularity

For the Argos mechanism, from the discussion above we can see that when the determinants of matrices **A** and **B** are equal to zero simultaneously, the singularity of type III occurs. Moreover, the constraint equation given by eq. (3) degenerates.

6. Conclusion

Singularity loci for spherical 3-DoF parallel manipulators with a special architecture have been studied for the first time in this paper. The concise analytical expressions describing the singularity loci of the manipulators have been derived using the solutions of the direct and inverse kinematic problems. These expressions have been used to obtain plots of the singularity curves and surfaces of the manipulators. For this manipulator, the three types of singularities have been discussed. It is noticed that, for this manipulator, four of the eight solutions to the direct kinematics are always the same. Furthermore, these four solutions correspond to the four singular configurations that exist in the Cartesian space. In other words, the singularity locus for this spherical manipulator in the Cartesian space consists of only four isolated configurations. In the joint space, the singularity locus is the regular surface described by eq. (17) with the period π. This result is due to the fact that, for each of the four singular Cartesian configurations, the actuators are freely movable (singularity of type III). All these results contrast with what is obtained for a general architecture in which at least one of the link angles is not equal to $\pi/2$. Hence, the orthogonal architecture is very attractive since it leads to tremendous simplifications and reduces the singularity locus to four isolated configurations in the Cartesian space. It can also be shown that the singularity locus is the same for any branch of the inverse kinematic problem, which is not true for arbitrary link parameters. Finally, it has been shown that the results obtained here also apply to the Argos manipulator, a spherical parallel manipulator based on pantographs.

Acknowledgment

The authors would like to acknowledge the help of Gabriel Côté with the fifth and the sixth figures.

References

Agrawal, S. K. 1991. Study of an in-parallel mechanism using reciprocal screws. *Proc. 8th World Congress on TMM*, Prague, Czechoslovakia, 405–408.

Asada, H., and Cro Granito, J. A. 1985. Kinematic and static characterization of wrist joints and their optimal design. *Proc. IEEE Int. Conf. on Robotics and Automation*, March 1985, St Louis, Missouri, 244–250.

Bonev, I. A., and Gosselin, C. M. 2001. Singularity loci of planar parallel manipulators with revolute joints. *Second Workshop on Computational Kinematics*, May 20–22 2001, Seoul, South Korea, 291–299.

Carretero, J. A., Podhorodeski, R. P., Nahon, M. A., and Gosselin, C. M. 2000. Kinematic analysis and optimization of a new three-degree-of-freedom spatial parallel manipulator. *ASME J. Mech. Des.* 122(1):17–24.

Cox, D. J., and Tesar, D. 1989. The dynamic model of a three-degree-of-freedom parallel robotic shoulder module. *Proc. 4th Int. Conf. on Advanced Robotics*, June 1989, Columbus, 475–487.

Craver, W. M. 1989. Structural analysis and design of a three-degree-of-freedom robotic shoulder module. Master's Thesis, The University of Texas at Austin, Department of Mechanical Engineering.

Fang, Y. F., and Huang, Z. 1997. Kinematics of a three-degree-of-freedom in-parallel actuated manipulator. *Mech. Mach. Theory* 32(7):789–796.

Gosselin, C., and Angeles, J. 1989. The optimum kinematic design of a spherical three-degree-of-freedom parallel manipulator. *ASME Trans., J. Mech. Trans. Autom. Des.* 111:202–207.

Gosselin, C., and Angeles, J. 1990. Singularity analysis of closed-loop kinematic chains. *IEEE Trans. Robot. Autom.* 6:281–290.

Gosselin, C., and Gagné, M. 1995. A Closed-form solution for the direct kinematics of a special class of spherical three-degree-of-freedom parallel manipulators. *Proc. 2nd Workshop on Computational Kinematics*, September 1995, Sophia Antipolis, France, 231–240.

Gosselin, C., and Hamel, J. 1994. The agile eye: A high-performance three-degree-of-freedom camera-orienting device. *Proc. IEEE Int. Conf. on Robotics and Automation*, May 1994, San Diego, 781–786.

Gosselin, C. M., and Lavoie, E. 1993. On the kinematic design of spherical 3-DoF parallel manipulators. *Int. J. Robot. Res.* 12(4):394–402.

Gosselin, C. M., Lemieux, S., and Merlet, J. P. 1996. A new architecture of planar three-degree-of-freedom parallel manipulator. *Proc. IEEE* 3738–3743.

Gosselin, C. M., Sefrioui, J., and Richard, M. J. 1992. On the direct kinematics of general spherical 3-DoF parallel manipulator. *Proc. ASME Mech. Conf.* 7–11.

Gosselin, C., and Wang, J. 1997. Singularity loci of planar parallel manipulators with revolute actuators. *J. Robot. Auton. Syst.* 21:377–398.

Hunt, K. H. 1983. Structural kinematics of in-parallel actuated robot arms. *ASME Trans., J. Mech. Trans. Autom. Des.* 105:705–712.

Lee, K. M., and Arjuman, S. 1991. A 3-DoF micromotion in-parallel actuated manipulator. *IEEE Trans. Robot. Autom.* 7(5):634–640.

Lee, K. M., and Shah, D. K. 1987. Kinematic analysis of a three-degree-of-freedom in-parallel actuated manipulator. *Proc. IEEE Int. Conf. on Robotics and Automation* 1:345–350.

Pfreundschuh, G. H., Kumar, V., and Sugar, T. H. 1991. Design and control of a three-degree-of-freedom in-parallel actuated manipulator. *Proc. IEEE Int. Conf. on Robotics and Automation* 1659–1664.

Sefrioui, J., and Gosselin, C. 1993. Singularity analysis and representation of planar parallel manipulator. *J. Robot. Auton. Syst.* 10:209–224.

Sefrioui, J., and Gosselin, C. 1994. Étude et représentation des lieux de singularité des manipulateurs parallèles sphériques à trois degrés de liberté avec actionneurs prismatiques. *Mech. Mach. Theory* 29:559–579.

Sefrioui, J., and Gosselin, C. 1995. On the quadratic nature of the singularity curves of planar three-degree-of-freedom parallel manipulators. *Mech. Mach. Theory* 30:533–551.

Song, S. M., and Zhang, M. D. 1995. A study of reactional force compensation based on three-degree-of-freedom parallel platforms. *J. Robot. Syst.* 12(12):783–794.

Vischer, P., and Clavel, R. 2000. A novel 3-DoF parallel wrist mechanism. *Int. J. Robot. Res.* 19(1):5–11.

Waldron, K. J., Raghavan, M., and Roth, B. 1989. Kinematics of a hybrid series-parallel manipulation system. *Trans. ASME, J. Mech. Transm. Autom. Des.* 111:211–221.

Zlatanov, D., Fenton, R. G., and Benhabib, B. 1994. Singularity analysis of mechanisms and manipulators via a motion-space model of the instantaneous kinematics. *Proc. IEEE Int. Conf. on Robotics and Automation*, May 1994, San Diego, 986–991.